Pergamon

Journal of Structural Geology, Vol. 16, No. 6, pp. 769 to 779, 1994

0191-8141/94 $07.00+0.00

The influence of structural lithic units in fault-related folds, Seminoe Mountains, Wyoming, U.S.A.

JOVITA B. DOMINIC and DAVID A. MCCONNELL

Department of Geology, University of Akron, Akron, OH 44325-4101, U.S.A.

(*Received* 8 *December* 1992; *accepted in revised form* 9 *August* 1993)

Abstract—Analysis of basement-involved folds in the Seminoe Mountains, south-central Wyoming, reveals that lithological contrasts within the sedimentary section created a mechanical anisotropy that influenced both fault geometry and the relative rates of fault propagation and fault slip. Two structural lithic units are identified, a competent lower unit and an overlying incompetent unit. The upper unit is made up of moderate ductility rocks that were thinned ahead of the Hurt Creek fault. Offset formations in the upper unit have small relative stretch (ε_r) values and are interpreted to have represented an impediment to fault growth. In contrast, fault propagation was rapid relative to fault slip in the competent rocks of the lower structural lithic unit which have a correspondingly higher relative stretch.

The Black Canyon fault is oriented at a low-angle to bedding in the lower structural lithic unit and is layer-parallel near the base of the upper unit. The Red Spring fault is a thin-skinned thrust fault and is interpreted to be linked to the Black Canyon fault to generate a triangle-zone geometry. Similar structures can be identified elsewhere in the Rocky Mountain foreland and this configuration may represent a previously unrecognized indicator of low-angle basement faults.

Changes in the deformation style between structural lithic units must be reflected in changing fold form, thus preventing the direct application of geometric and kinematic models that predict a uniform fold profile.

INTRODUCTION

BASEMENT faults in the Seminoe Mountains either lose displacement upsection into folds, or change orientation up-dip to become parallel to bedding. Similar structural relationships are recognized in fault-propagation and fault-bend folds, respectively, in thrust-and-fold belts (Boyer 1986, Jamison 1987, Mitra 1990). Deformation within fault-related folds is dependent upon fault angle and fold shape and can be predicted by geometric and kinematic modeling (Suppe & Medwedeff 1984, 1990, Jamison 1987, Mitra 1990). Kinematic models developed to examine such fold styles assume that rocks in the hanging wall of the fault are transported along a bedding-parallel thrust flat. The absence of similar detachment planes in most basement rocks precludes the application of these models to analyze basement-involved, fault-related folds. Alternative interpretations of fault evolution in which the thrust fault nucleates as a ramp (Eisenstadt & De Paor 1987) may be more applicable to structures involving basement rocks (Chester & Chester 1990).

Several kinematic models have been created specifically to analyze basement-involved folds. These models assume a variety of configurations, including: (i) folds formed above fault zones of variable width (Spang *et al.* 1985); (ii) folds formed above discrete reverse faults (Erslev 1991, McConnell & Wilson 1993); and (iii) hybrids of both styles (Narr & Suppe 1989, Schmidt *et al.* 1993). Several models used to analyze basement-involved folds share the implicit assumption that fold hinges migrated during folding (Narr & Suppe 1989, Chester & Chester 1990, Schmidt *et al.* 1993, McConnell & Wilson 1993), however, few have addressed this aspect of folding directly. In addition, some models show deformation in cover rocks accommodated exclusively by folding and thickness changes as slip increased on an underlying basement fault (or group of faults; Spang *et al.* 1985, Narr & Suppe 1989, Erslev 1991). Basement faults in natural folds are more accurately represented in models that incorporate faults which propagate upsection into cover rocks (Chester & Chester 1990, McConnell & Wilson 1993). Regardless of the details of individual models, they are all used to predict the kinematic evolution of folds based upon the geometric form of idealized structures; they cannot be used to assess how mechanical anisotropies within the sedimentary section influence the folding process.

An alternative procedure for the examination of fault–fold relationships involves consideration of the relative rates of fault slip and fault propagation. Folding of rocks ahead of a propagating fault has been viewed as the passage of a ductile bead through the deformed rocks (Williams & Chapman 1983). A comparison of the relative magnitudes of fault slip (d) and fault propagation length (l_f) reveals how much deformation must have occurred within folded units ahead of the fault tip (Fig. 1) (Williams & Chapman 1983, Chapman & Williams 1984). The contrast between deformation within the hanging wall and footwall units is modest where fault slip is small relative to fault propagation length (Fig. 1d), whereas there must be substantial internal deformation in beds that exhibit large offsets relative to the length of the fault (Figs. 1b & c). Chapman & Williams (1984) defined a value, relative stretch (ε_r, Fig. 1), which represents a measure of the relative strains in the faulted

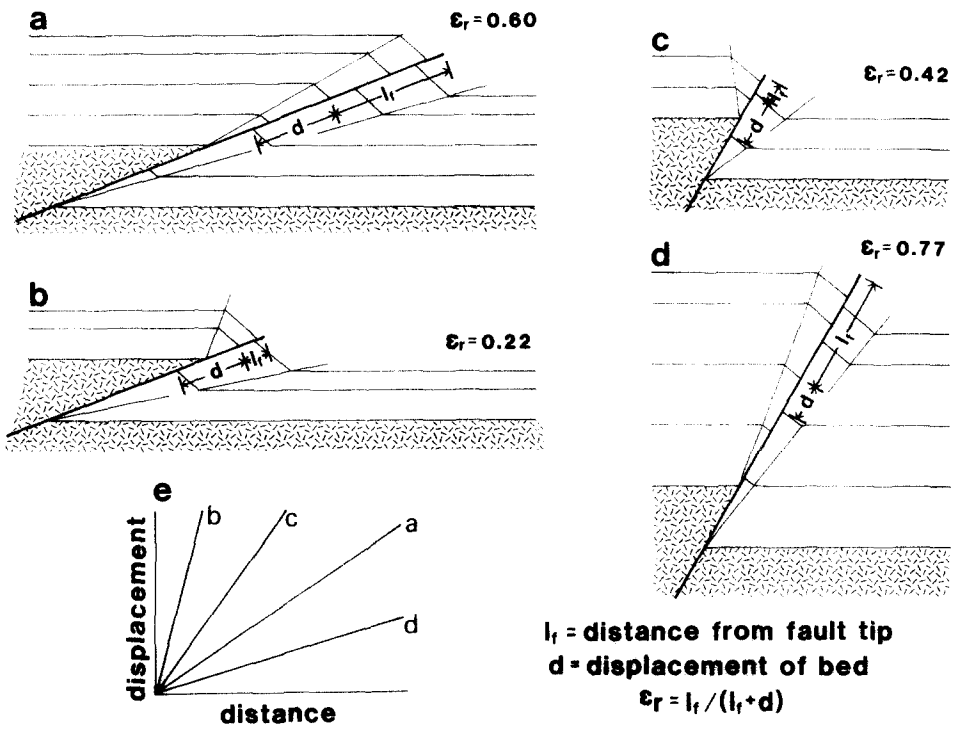

Fig. 1. Relationship between fault displacement (d), fault propagation length (l_f) and deformation in fault-related folds. All folds have an interlimb angle of 140° and all configurations are balanced by area. Relative stretch (ε_r) is large where most shortening is accommodated by fault slip (a & d), and small where deformation is accommodated by fault slip (a & d), and small where deformation is accommodated by folding and thickness changes (b & c). (a) Fault angle = 20°, $l_f > d$, $\varepsilon_r = 0.6$; (b) fault angle = 20°, $l_f < d$, $\varepsilon_r = 0.22$; (c) fault angle = 60°, $l_f < d$, $\varepsilon_r = 0.42$; (d) fault angle = 60°, $l_f > d$, $\varepsilon_r = 0.77$; (e) plot of distance (l_f) vs fault displacement (d) for the four configurations shown.

units. Small ε_r values (<0.5, Figs. 1b, c & e) occur if the fault propagation rate is small relative to the rate of fault slip, thus requiring unfaulted beds to shorten by folding and internal deformation (Williams & Chapman 1983). In contrast, large ε_r values (>0.5) would be generated where a fault propagates rapidly in comparison with fault slip. In this case fault length would greatly exceed fault slip (Figs. 1a, d & e) and strains in the folded units would be relatively small.

This paper examines well-exposed fault–fold relationships in the Seminoe Mountains where two basement faults lose displacement up-section into folds. We link macroscopic and mesoscopic structures to constrain interpretations of the evolution of folds that formed ahead of propagating faults. We demonstrate that the observed deformation patterns depart from configurations predicted by simple kinematic models because of mechanical anisotropies in the sedimentary rocks. The base-

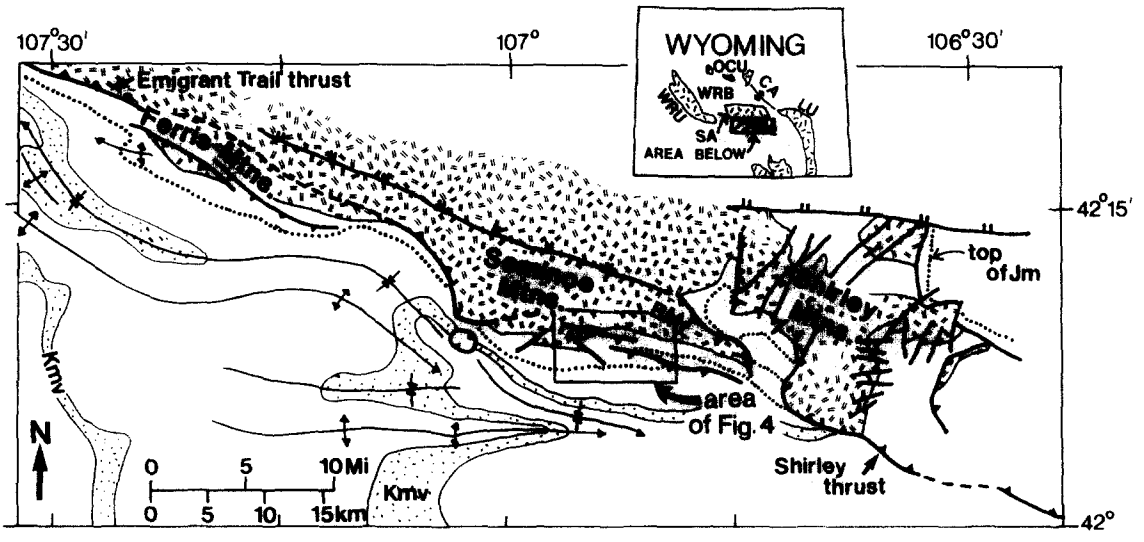

Fig. 2. Geology of southern margin of the Sweetwater Arch (present day Granite Mountains), after Blackstone (1983) and Bergh & Snoke (1992). Abbreviations in inset map: CA = Casper Arch; LU = Laramie Uplift; OCU = Owl Creek Uplift; SA = Sweetwater Arch; WRB = Wind River Basin; WRU = Wind River Uplift. Abbreviations for main map: BMf = Bennett Mountain fault; Jm = Morrison Formation; Kmv = Mesaverde Formation.

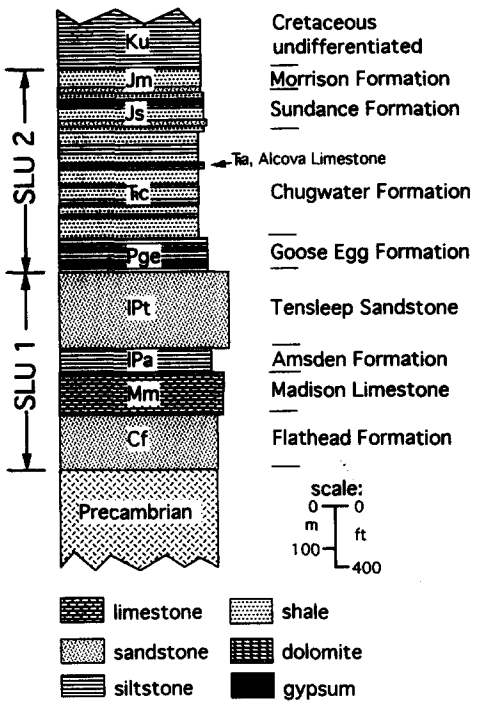

Fig. 3. Simplified stratigraphic column of rocks mapped in the southern Seminoe Mountains. SLU = structural lithic unit.

ment rocks discussed herein may be analogous to the competent sedimentary rocks in which thrust ramps nucleate (Eisenstadt & De Paor 1987). Consequently, the conclusions of this study may be applicable to folds beyond the Rocky Mountain foreland province.

STUDY AREA

The study area is in the Seminoe Mountains, on the southern margin of the Granite Mountains, south-central Wyoming (Fig. 2). Precambrian rock exposures in the Rocky Mountain foreland are collectively referred to as basement (Brown 1988). Basement in the Seminoe Mountains is made up primarily of alkali feldspar granite, leucogranite and granite. The oldest rock is a gneissic granite, with a strong SE-dipping foliation and associated with the gneissic granite are amphibolite bodies which trend 070–120°. Common diabase dikes range in width from a few centimeters to several meters and show a consistent northeast strike (0–050°).

Overlying basement is a sedimentary section of the Cambrian Flathead to Pennsylvanian Tensleep Formations (Hausel & Jones 1984) (Fig. 3). With the exception of the relatively thin Amsden Formation, these formations consist of competent, low-ductility sandstones and limestones. The Permian Goose Egg Formation and younger rocks (Fig. 3) are less competent, moderate-ductility siltstones and shales. We believe these two

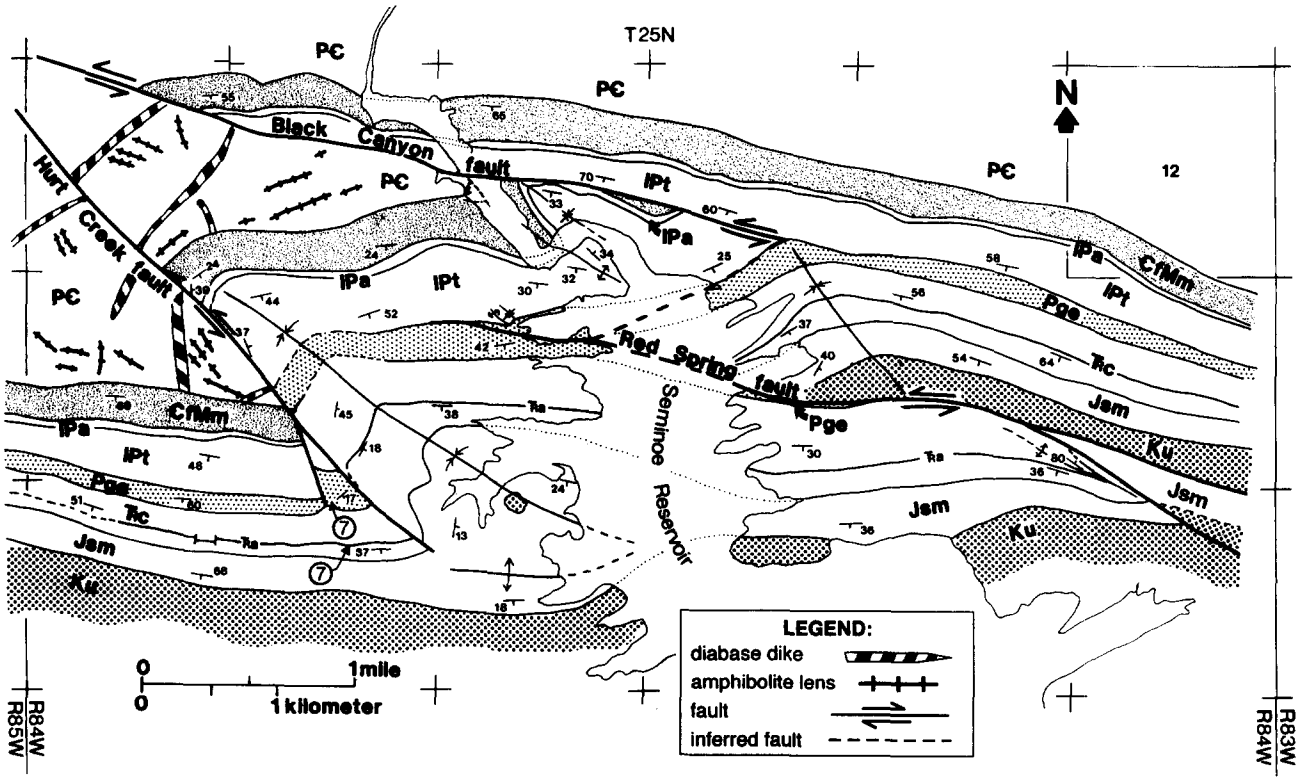

Fig. 4. Geologic map of study area. P€ = Precambrian rocks; €fMm = Flathead Formation–Madison Formation; IPa = Amsden Formation; IPt = Tensleep Formation; Pge = Goose Egg Formation; Tc = Chugwater Formation; Ta = Alcova Limestone Member; Jsm = Sundance and Morrison Formation; Ku = undifferentiated Cretaceous rocks. Circled numbers show locations of features illustrated in Fig. 7.

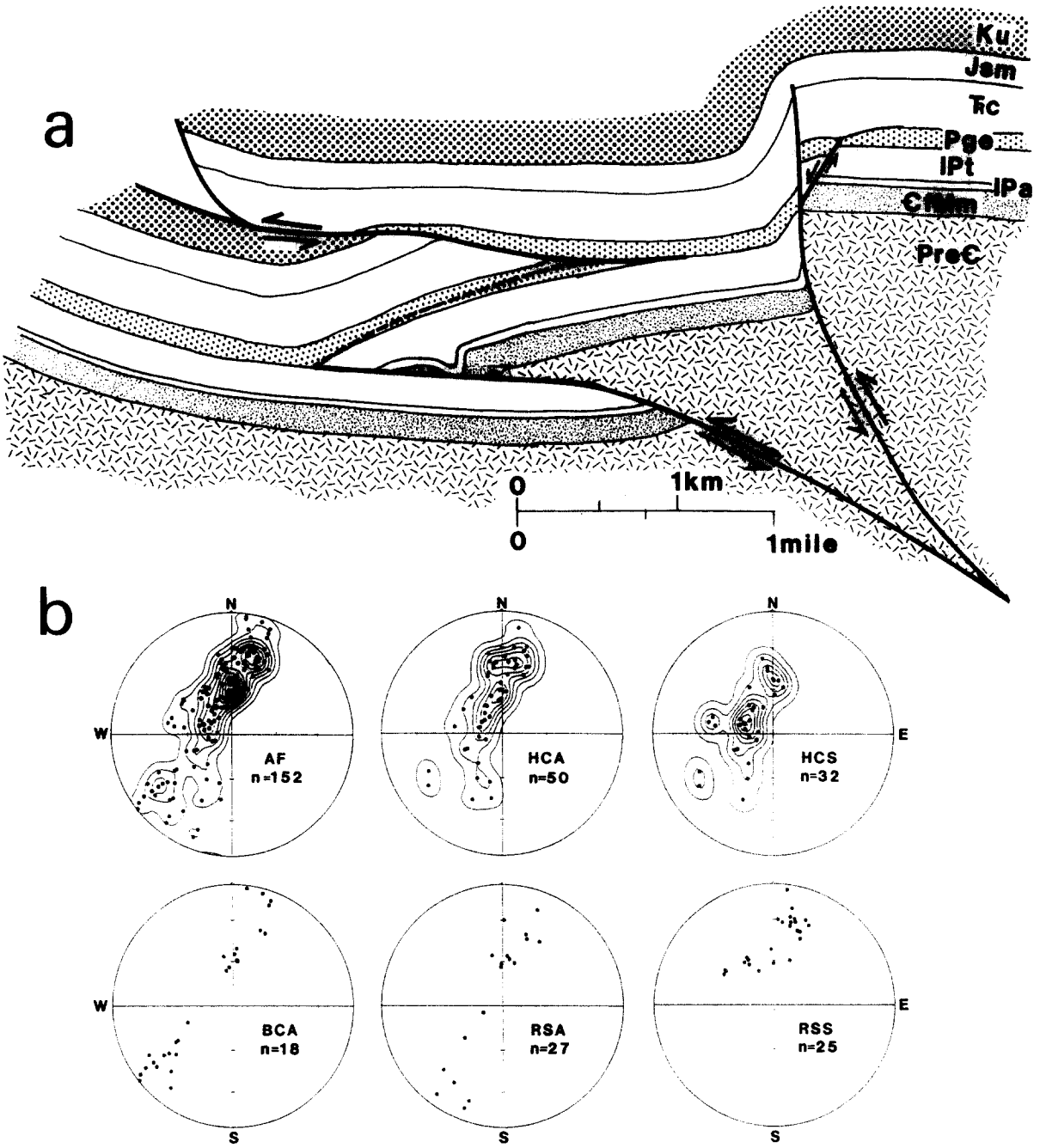

Fig. 5. Down-plunge projection and fold orientations. (a) Down-plunge projection of geologic map; (b) lower-hemisphere, equal-area projections of poles to bedding in folds, n = number of measurements per plot. Plots contoured (if $n > 30$) using Kamb method for a contour interval of 2σ, first contour = 2σ. AF = combined data from all folds; HCA = Hurt Creek anticline (in sections 20 and 21); HCS = Hurt Creek syncline (sections 16, 17 and 21); BCA = Black Canyon anticline (section 9); RSA = Red Spring anticline (sections 13 and 14); RSS = Red Spring syncline (sections 14 and 15).

sections of sedimentary rocks can be considered as separate structural lithic units (Currie *et al.* 1962).

The sedimentary rocks dip steeply (50–70°) southward over much of the area, except where disrupted by three plunging structures, the Hurt Creek, Black Canyon (Shoemaker 1936, Cooper 1951, Allspach 1955) and Red Spring faults (Fig. 4). As a consequence of the steep inclination of the sedimentary rocks, the map pattern can be viewed as an oblique cross-section through the structures of the area. A down-plunge projection of the map area was constructed to remove geometric distortions inherent in the map view (Fig. 5a) and this projection was used in combination with the field data to interpret the deformation history. The down-plunge projection was constructed using an average plunge and azimuth value for principal fold axes (20°, 125°) which have a consistent orientation throughout much of the area (Fig. 5b).

FAULT–FOLD RELATIONSHIPS

Hurt Creek fault

The Hurt Creek fault is a high-angle reverse fault with a maximum strike-separation of 1.5 km at the basement–

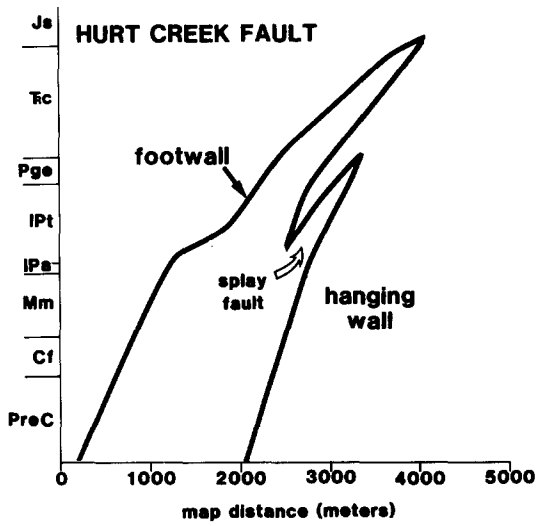

Fig. 6. Stratigraphic separation diagram for Hurt Creek fault. Stratigraphic abbreviations given in Fig. 3. Map distance represents distance measured along fault trace from fault tip.

cover interface, decreasing to zero at a tip line located in Jurassic rocks (Figs. 4 and 6). Associated with this up-section decrease in separation is a corresponding change in fold geometry: the basement–cover interface is planar, the Cambrian to Pennsylvanian section exhibits only minor footwall folding, and the fold is accentuated in Permian to Jurassic rocks in both the hanging wall and footwall (Figs. 4 and 5). This sequence, in which faulting is replaced by folding up-section, is similar to that recognized in thin-skinned fault-propagation folds (Suppe & Medwedeff 1984, 1990).

The mesoscopic features associated with the Hurt Creek fault indicate extension of beds near the fault. The outcrop width of the Goose Egg Formation narrows from 140 m at the western edge of the map to 70 m at the tip of the minor splay fault (Fig. 4), despite a uniform dip. Mesoscopic faults with normal offsets are present in road-cuts of Chugwater (Fig. 7a) and Goose Egg (Fig. 7b) formations southwest of the fault (Fig. 4). The majority of these minor faults are inclined (50–80°) to the northeast (Fig. 7) and exhibit dip-separations of less than 4 m. Outcrops of Chugwater Formation in a stream valley adjacent to the fault to the northeast do not contain mesoscopic faults.

The upper Sundance Formation and younger units are deformed into an E-plunging anticline southeast of the fault tip. A complementary syncline is located northeast of the fault (Fig. 4). The hingeline of the syncline intersects the fault at the basement–cover contact, whereas the anticline's hingeline intersects the fault near the fault tip (Fig. 4). The syncline hinge is tight and angular as outlined by the Tensleep Sandstone and the Alcova Member of the Chugwater Formation (Fig. 4).

Black Canyon fault

The Black Canyon fault (Fig. 4) places basement rocks against lower Paleozoic rocks. Strike-separation measured at the base of the Flathead is approximately 3 km, and decreases to the east; there is no offset of stratigraphic units younger than Pennsylvanian age.

The location of the Black Canyon fault can be estimated from the juxtaposition of sedimentary rocks that crop out in steep slopes along the shores of the reservoir near the northern boundary of the study area. The approximate orientation of the fault plane is N83°W

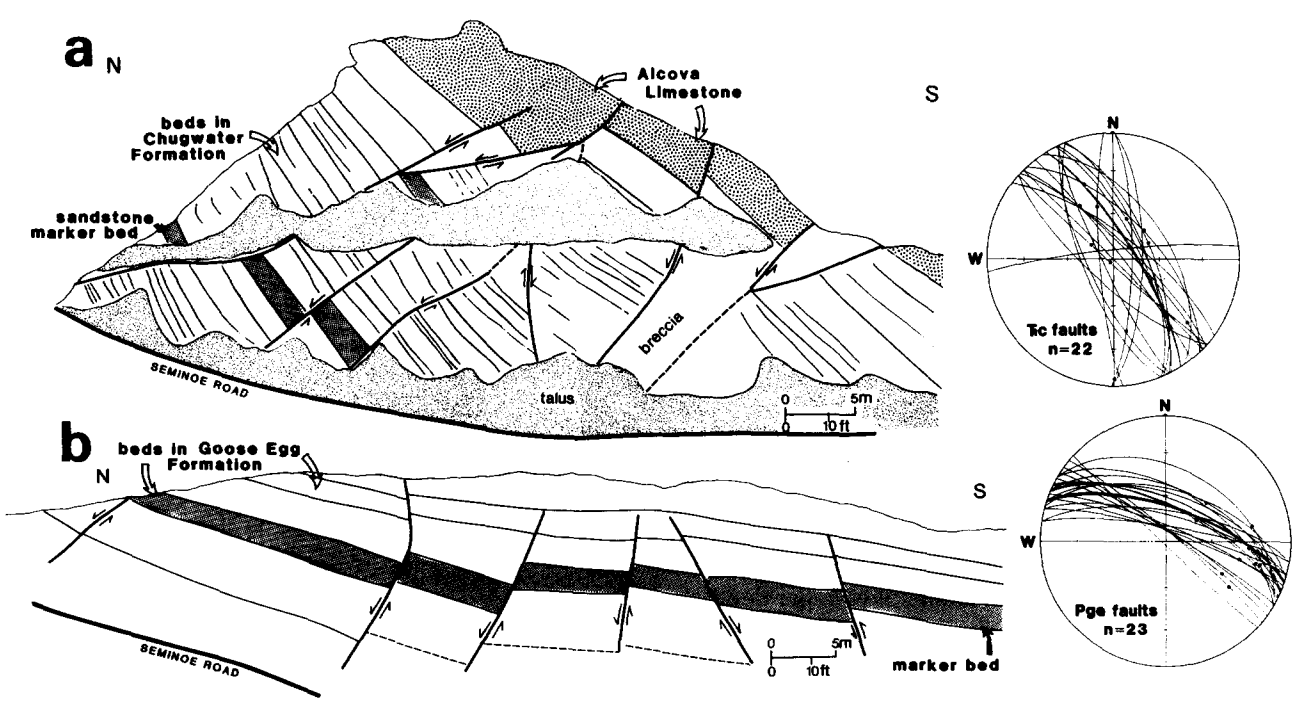

Fig. 7. Minor faults in road-cuts along Seminoe Road. Locations of road-cuts shown on Fig. 4. Stereonets are lower-hemisphere, equal-area projections of fault great circles, n = number of measurements per plot. Black dots show orientations of slickenside lineations. (a) Chugwater Formation, majority of faults (20) have normal separation, approximately half have slickensides that indicate normal- or oblique-slip; (b) Goose Egg Formation, almost all faults (22) exhibit normal separation and approximately half have a recognizable component of right slip.

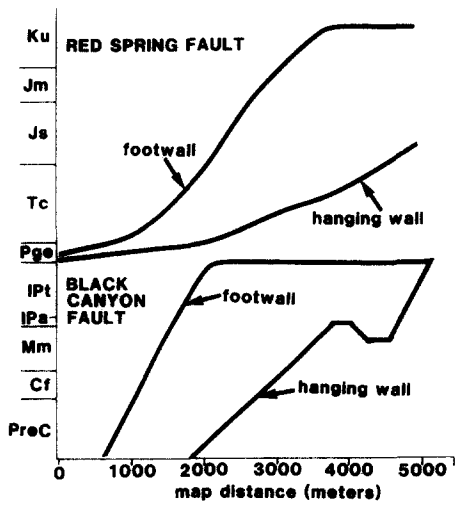

Fig. 8. Stratigraphic separation diagrams for Black Canyon and Red Spring faults. Abbreviations given in Fig. 3. Map distance represents distance measured along fault trace from fault tip.

53°SW, subparallel to bedding north of the fault (Fig. 4) using structure contours. The down-plunge projection (Fig. 5) shows the Black Canyon fault as a low-angle basement fault. Shortening of basement rocks occurred by offset on the fault and required broad folding and rotation of the hanging wall as it moved from the footwall ramp onto the footwall flat.

A fold pair is outlined in Mississippian and Pennsylvanian rocks adjacent to the tapered end of the wedge of basement south of the Black Canyon fault. The hinge lines of the fold pair intersect the fault near the basement–cover contact (Fig. 4). The folds formed prior to the fault as the fault cuts the northern fold limb (Fig. 4).

Shortening of Permian through Cretaceous rocks occurred by displacement on the Red Spring fault. The Red Spring fault was referred to as the Bennett Mountain fault by Allspach (1955), but recently this name has also been applied to a large basement-involved fault northeast of the study area (Bergh & Snoke 1992). To avoid confusion we use the name Red Spring fault for Allspach's Bennett Mountain fault.

Unlike the Hurt Creek and Black Canyon faults, the Red Spring fault decreases in separation down-section, and does not offset units older than the Permian Goose Egg Formation which is doubled in thickness on the western shore of the reservoir (Fig. 4). The fault places Goose Egg and Chugwater Formations over Cretaceous rocks on the eastern shore (Fig. 4), and fault stratigraphic separation increases to the east (Fig. 8). Structural relations across the fault cannot be readily determined in the easternmost part of the map area where the fault is concealed beneath younger deposits.

The Black Canyon and Red Spring faults are interpreted to be linked by an antithetic detachment fault that extends southwest from the tip of the Black Canyon fault within the Goose Egg formation (Figs. 4 and 5). Displacement must be transferred from the Black Canyon fault to the Red Spring fault to conserve bed length and thus ensure a balanced structural configuration. A possible alternative interpretation would be that the Black Canyon fault continues to the east within the Goose Egg formation and ramps up-section outside the map area. However, this pattern cannot be recognized on geological maps (Allspach 1955), and it does not provide an explanation for the presence of the Red Spring fault.

The following kinematic evolution is proposed for the Black Canyon and Red Spring faults (Fig. 9). Deformation began as the Black Canyon fault cut up-section from Precambrian rocks into the overlying sedimentary section. The Black Canyon fault became layer-parallel at the top of the Tensleep–base of Goose Egg (Fig. 9b). Shortening of Flathead–Tensleep rocks occurred by displacement on the Black Canyon fault. In contrast, upper Paleozoic and Mesozoic rocks were not cut by this fault but were shortened by slip on the Red Spring fault. This created a triangular fault zone geometry (Fig. 9b) similar to triangle zones observed at the foreland edge of thrust belts (Charlesworth & Gagnon 1985). The hanging wall ramp of the Black Canyon fault lies in the footwall of the antithetic fault which shows an opposing sense of vergence. As displacement increased on the Black Canyon fault, slip on the associated antithetic fault and red Spring fault also increased (Fig. 9c).

The Hurt Creek and Red Spring fault planes do not crop out in the study area, thus we are unable to definitively constrain their sense of slip. A small portion of the Black Canyon fault plane is accessible at the reservoir shore in eastern section 8 (Fig. 4). Minor faults in the adjacent Tensleep Sandstone have a consistent southwest dip and approximately half display slickenlines (Fig. 10), all of which are indicative of dip-slip movement. Stratigraphic relations and occasional slickensides indicate that displacements on some of these faults were reverse. Both beds and faults are steeply inclined, therefore, slip is subparallel to bedding. Approximately half the minor faults in the hanging wall of the Hurt Creek fault were normal- or oblique-slip faults (Fig. 7), however, it is unclear if these faults were directly related to the Hurt Creek fault or were formed during folding. Minor faults associated with NW-striking basement faults in the nearby Shirley Mountains (Fig. 2) exhibit displacements with components of reverse-slip and strike-slip (Bergh & Snoke 1992). Regardless of their sense of slip, faults propagated up-section from massive basement rocks into layered sedimentary rocks, and mechanical anisotropies within the cover rocks are interpreted to have influenced the geometry of the resulting structures.

DISCUSSION

Placement of basement faults

Amphibolite lenses exhibit a northwest trend (Fig. 4) in the hanging wall of the Hurt Creek fault. Trends in the hanging wall of the Black Canyon fault exhibit more variety, ranging from 50° to 150° (Fig. 4). Diabase dikes

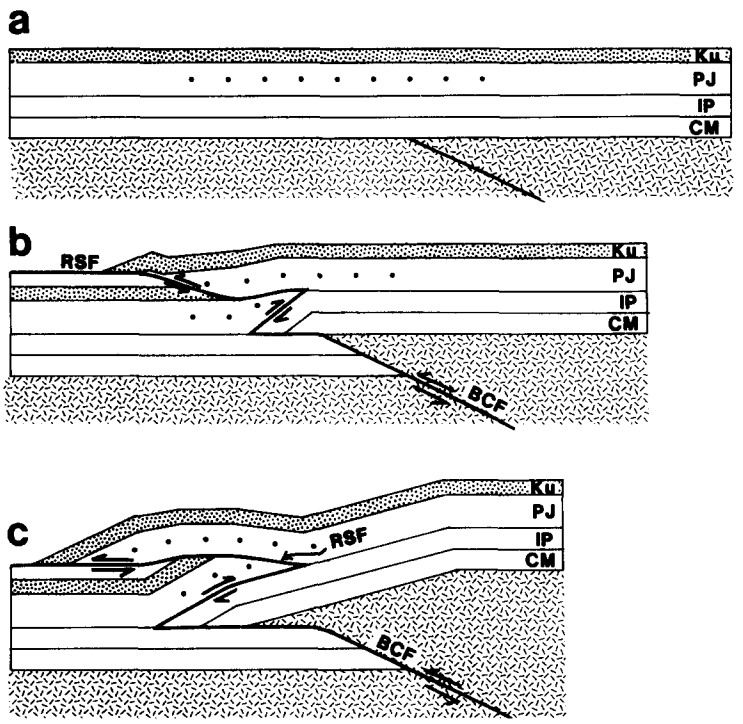

Fig. 9. Simplified schematic diagram for evolution of structures along the southern flank of Seminoe Mountains.

are offset across the Hurt Creek fault by the same amount of strike-separation as seen on the basement–cover contact. Diabase dikes strike northeast and are subparallel to an additional fault, the Indian Spring fault, located 2 km west of the map area. Foliations in the gneissic granites also strike northeast and dip steeply to the northwest. The similarity between the orientations of basement fabrics and Laramide faults suggest that the Laramide structures may represent the reactivation of Precambrian fabrics, or that the fabrics in basement rocks acted as strain guides for the younger deformation (Bergh & Snoke 1992). Schmidt *et al.* (1993) and Miller & Lageson (1993) documented a similar correspondence between Precambrian features and Laramide fault zones in basement-involved folds throughout the Rocky Mountain foreland.

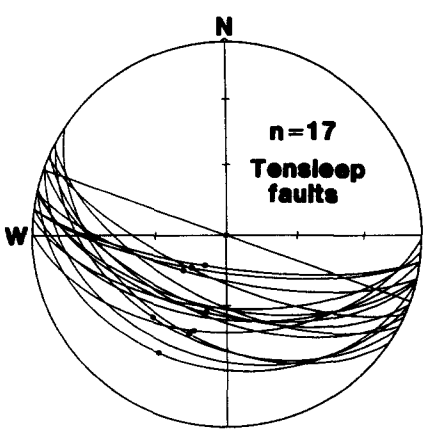

Fig. 10. Minor faults in Tensleep Sandstone adjacent to Black Canyon fault. Lower hemisphere, equal-area projection of fault great circles, n = number of faults, black dots show orientations of slickenside lineations.

Fault–fold interaction

Normalized displacement–distance plots illustrate variations in mechanical stratigraphy. A normalized plot would yield a straight line with a 45° slope (Fig. 11a) where the ratio of displacement to distance remained uniform along the fault. In contrast, a curvilinear plot would indicate a change in the relative rates of fault propagation and fault slip (Figs. 11b & c). A gentle slope indicates that fault length increased rapidly relative to fault displacement, whereas a steep slope reflects a fault which grew slowly relative to displacement (Figs. 1 and 11). The relationship between displacement and fault length is influenced by the mechanical properties of the faulted rocks (Muraoka & Kamata 1983, Cowie & Scholz 1992), therefore, the shape of the curve may reflect mechanical contrasts within the faulted units. Muraoka & Kamata (1983) noted that displacement on faults decreased rapidly relative to fault length as a fault passed from a rigid competent layer into surrounding incompetent rocks. They proposed that incompetent rocks acted as strain absorbers in which fault displacement was replaced by other deformation mechanisms. One explanation of a concave-upward plot is that a competent unit lies above an incompetent layer (Fig. 11b); a concave-downward plot would be generated where a competent unit underlies incompetent rocks (Fig. 11c). The degree of curvature of the plots would increase with increasing ductility contrast (Figs. 11b & c). The curvature may also be influenced by the nature of the contact between structural lithic units.

Structural lithic units are typically defined based upon the average properties of rocks in a given stratigraphic interval (Currie *et al.* 1962). Individual formations, members or beds within the interval may be more or less

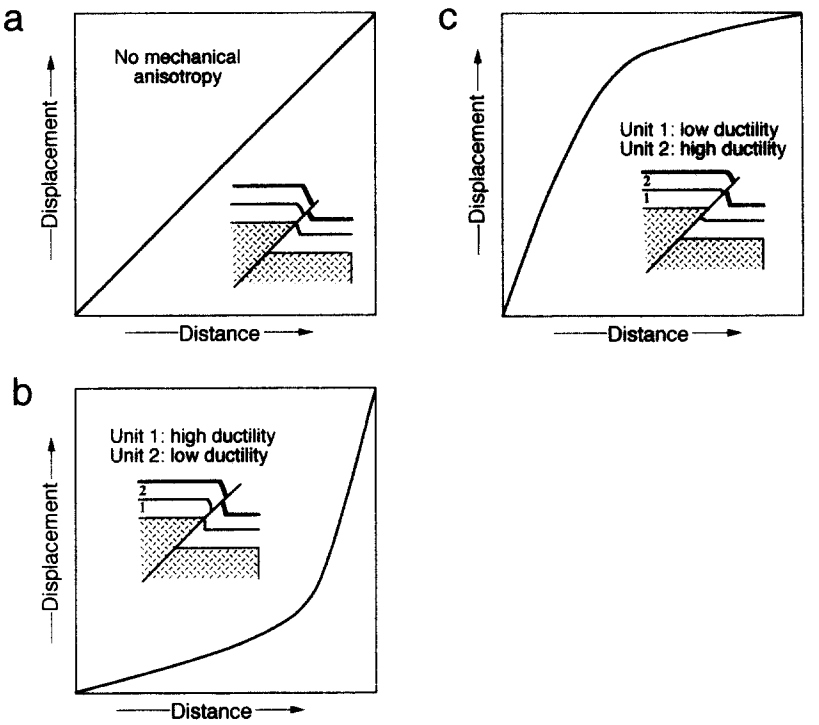

Fig. 11. Schematic displacement vs distance diagrams illustrating influence of mechanical stratigraphy on the shape of the plot. (a) No mechanical anisotropy; (b) incompetent (high ductility) lower structural lithic unit, competent (low ductility) upper unit; and (c) competent lower unit, incompetent upper unit.

competent than the unit as a whole. As a fault propagates up-section into an overlying structural lithic unit, the transition from one unit to the next will depend upon the mechanical contrast between the rocks at the top of the lower unit and the base of the upper unit. The relative rates of fault displacement and fault propagation may change as a fault cuts across a sharp contact between units; this would be represented by two straight line segments on a displacement–distance plot (Fig. 12). In contrast, the relative rates of displacement and propagation would change gradually if there is a gradational transition between structural lithic units; this would yield a curvilinear plot (Fig. 12).

Sedimentary rocks in the study area exhibit a contrast in deformation styles and, on this basis, are subdivided into two structural lithic units (Fig. 3). Unit 1 is composed of competent Cambrian–Pennsylvanian rocks and

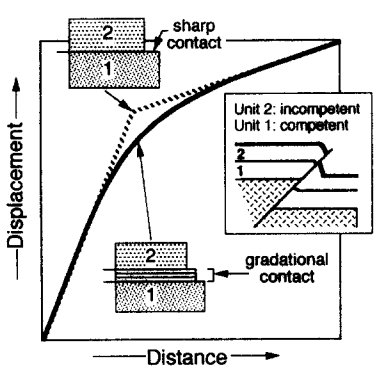

Fig. 12. Schematic displacement vs distance diagram illustrating influence of the boundary between structural lithic units on the shape of the plot. Straight-line plot indicates a distinct contact is present between units; a curvilinear plot indicates gradational transition zone.

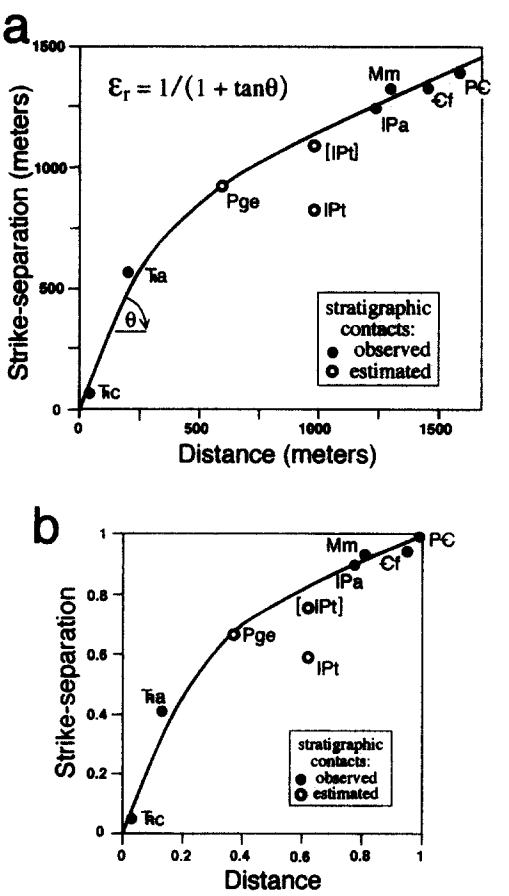

Fig. 13. Strike-separation vs distance plot for the Hurt Creek fault. Separations of Tensleep and Goose Egg Formations are estimated as these units crop out discontinuously adjacent to the fault in the footwall. Tensleep point in brackets represents sum of separations on the Hurt Creek fault and adjoining fault splay. Stratigraphic abbreviations are the same as in Fig. 4.

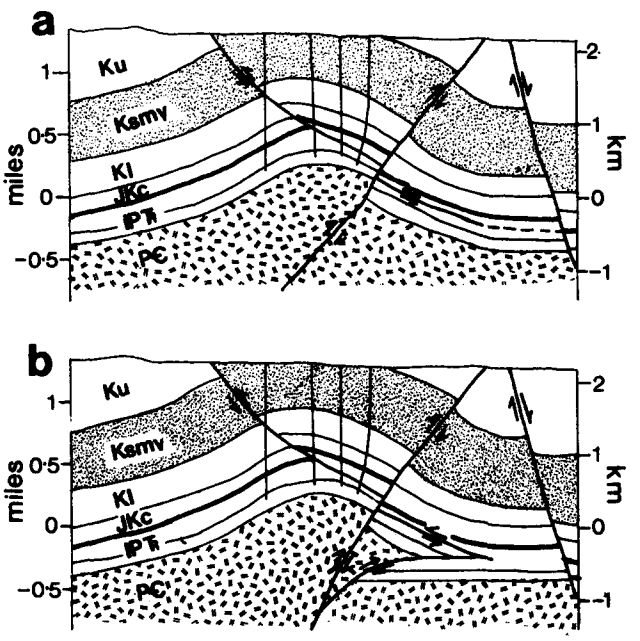

Fig. 14. Interpretation of interaction of thin-skinned thrust fault with underlying basement fault at Quealy Dome, Laramie Basin, Wyoming: (a) original cross-section from Blackstone (1983); and (b) reinterpretation of structure with triangle zone geometry. P€ = Precambrian rocks; lPTr = Pennsylvanian–Triassic rocks; JKc = Jurassic–Cloverly Formation; Kl = Thermopolis Shale–Frontier Formation; Ksmv = Steele Shale and Mesaverde Formation; Ku = undifferentiated Cretaceous rocks.

Unit 2 is made up of the less competent Permian–Jurassic section. The lower unit accommodated shortening primarily by displacement on the Black Canyon and Hurt Creek faults, whereas the upper unit was shortened by a combination of displacement on the thin-skinned Red Spring fault and folding ahead of the Hurt Creek fault. We have chosen the boundary between structural lithic units to lie at the base the Goose Egg Formation. The Goose Egg contains interbedded shale, siltstone, gypsum, sandstone and limestone, and may actually represent a gradational contact between competent sandstones in the Tensleep and incompetent shales at the base of the Chugwater Formation.

Standard and normalized plots of strike-separation vs distance for the Hurt Creek fault show concave-downward curves with gentle slopes for formations in structural lithic unit 1 and steep slopes for rocks in unit 2 (Fig. 13). Fault length increased rapidly relative to fault displacement for unit 1 whereas the fault propagated more slowly relative to displacement in unit 2 (Fig. 13). Relative stretch can be determined from the slope (θ) of the standard plot (Fig. 12a) as

$$\varepsilon_r = 1/(1 + \tan\theta). \quad (1)$$

This yields a relative stretch of 0.64 for structural lithic unit 1 and $\varepsilon_r = 0.29$ for rocks of unit 2. The low value for unit 2 infers that these rocks underwent substantial deformation prior to the passage of the fault (Fig. 1). The less competent rocks of unit 2 are therefore considered to have represented an impediment to fault growth (Muraoka & Kamata 1983, Ellis & Dunlap 1988). A similar relationship has been documented at Dry Fork Ridge anticline, northern Bighorn Mountains (Hennings & Spang 1987), where a basement fault loses displacement up-dip into an anticline in a thick shale-dominated section of Cambrian rocks.

Structural lithic units can be identified in basement-involved fault-related folds throughout the Rocky Mountain foreland and represent mechanical anisotropies that will be overlooked if we focus entirely on the sequential geometric relationships typically represented by kinematic models. Fold shape must change in each structural lithic unit if each responds differently to the propagation of an underlying fault. The magnitude of the changes will depend upon the stratigraphic order of units, their relative thicknesses and their relative strengths. Incompetent units may hinder the passage of fault upsection, whereas, faults may nucleate in overlying competent units and eventually propagate downsection to coalesce with an underlying fault. Such faults would have segments with small offsets (in incompetent units) separating segments with larger offsets (competent units; Ellis & Dunlap 1988).

Both basement and sedimentary rocks are effectively uniform throughout the study area but macroscopic deformation patterns associated with the Hurt Creek and Black Canyon faults clearly differ. The contrast between the deformation styles associated with the Hurt Creek and Black Canyon faults is primarily a consequence of contrasting fault-bedding cut-off angles (Hurt Creek = high angle; Black Canyon = low angle). The distribution of mesoscopic structures in Permian and Triassic rocks in the hanging wall of the Hurt Creek fault is interpreted to suggest that thinning is heterogeneous and is most pronounced near the anticline's hinge. Similar patterns can be recognized above steep reverse faults elsewhere in the Rocky Mountains (e.g. Rattlesnake Mountain, Stearns 1971; Dry Fork Ridge anticline, Hennings & Spang 1987).

The absence of normal faults in the footwall (northeast) of the Hurt Creek fault indicates that rocks in the footwall and hanging wall did not share a common deformation path. A contrasting history for footwall and hanging wall deformation is interpreted to mean that fold hinges did not migrate through the forelimb, but were fixed in place during deformation. In addition, the fault cut through the anticline's hinge, whereas the syncline's hinge is unfaulted. These characteristics are not easily reconciled with some kinematic models which assume a mobile hinge and a fault that cut up-section through the syncline hinge zone (Suppe & Medwedeff 1984, 1990, Chester & Chester 1990; Schmidt *et al.* 1993). In contrast, this analysis of the Hurt Creek structure suggests that fold hinges were fixed, heterogeneous thickness changes occurred within folded units, and the relative rates of fault propagation and fault slip changed with stratigraphic level.

Significant shortening occurred when the Black Canyon fault became parallel to bedding up-section (Figs. 9b&c). Thrust faults such as the Red Spring fault are a kinematic consequence of slip on an underlying basement fault. The Black Canyon and Red Spring

faults are interpreted to share a common detachment horizon in the sedimentary section. The hanging wall of the basement fault represents a wedge that undercut the sedimentary section, effectively peeling off the sedimentary rocks above a bedding-parallel fault segment (Fig. 9).

A similar sequence of deformation has been proposed for the Moxa Arch, Wyoming (Kraig *et al.* 1988), and comparable configurations have been postulated for Rattlesnake Mountain and the Forellen fault, Wyoming (Erslev 1986), and the southern Bridger Range, Montana (D. Lageson personal communication 1993). Blackstone (1983) illustrated a thrust fault with an opposing sense of vergence to the underlying basement fault at Quealy Dome in the western Laramie basin, southeast Wyoming (Fig. 14a). The thrust fault lies at the same stratigraphic horizon as the Red Spring fault and is offset by a high-angle reverse fault similar to the Hurt Creek fault. The structure can be reinterpreted to mimic the macroscopic structures associated with the Black Canyon and Hurt Creek faults (Fig. 14b). Subsurface controls are not sufficient to rule out either interpretation, however, our interpretation provides a kinematic explanation for the presence of the bedding-parallel thrust fault.

Recognition of the styles and mechanisms of deformation for the Hurt Creek and Black Canyon structures provides constraints on future interpretations (or reinterpretations) or basement-involved folds in areas of southeastern Wyoming with similar stratigraphic units. These patterns will be modified where lithologic variations create different arrangements of structural lithic units.

CONCLUSIONS

Examination of structures along the southern flank of the Seminoe Mountains has revealed the following.

(1) Two basement-involved faults dominate the area, the Hurt Creek and Black Canyon faults. Contrasting patterns of deformation above the faults is a consequence of fault angle and mechanical contrasts between the structural lithic units in the cover rocks. Extensional structures are present in the hanging wall of the Hurt Creek fault which makes a high angle with bedding. In contrast considerable shortening occurred on the Red Spring fault associated with the low-angle Black Canyon fault.

(2) The map-scale structures associated with the Hurt Creek fault resemble a fault-propagation fold as the fault loses separation up-section into a fold. Previous fault-propagation fold models assumed migrating fold hinges; however, this analysis interprets fold hinges to be fixed in position early during fold evolution.

(3) The Black Canyon fault has a fault-bend fold geometry as the hanging wall was transported over a ramp onto a footwall flat. This combination of fault style and mechanical stratigraphy resulted in the development of a triangle-zone geometry seldom recognized in foreland folds. The presence of thin-skinned thrusts in basement-involved folds may signal the existence of both a basement fault that becomes layer-parallel up-section and separate structural lithic units in the cover rocks. The identification of these features will aid in the interpretation of other foreland structures.

(4) This analysis illustrates the need to take into account the mechanical interaction between a basement fault and the overlying cover rocks when modeling the evolution of basement-involved folds. Kinematic models may replicate the geometry of the faults and folds but they must be used with caution when attempting to predict the interaction of the fault with structural lithic units of contrasting mechanical properties. Displacement–distance plots are useful tools to identify contrasting mechanical units in fault-related folds.

(5) There is a general parallelism between Laramide faults and Precambrian basement fabrics, perhaps reflecting the reactivation of the latter. The Hurt Creek and Black Canyon faults are subparallel to amphibolite lenses, the neighboring Indian Spring fault parallels mafic dikes and gneissic foliations.

Acknowledgements—Reviews by D. Lageson and M. G. Rowan considerably improved the manuscript. L. M. Friberg assisted in mapping the Precambrian rocks. Acknowledgement is made to the Donors of The Petroleum Research Fund, administered by the American Chemical Society, for the support of this research.

REFERENCES

Allspach, H. G. 1955. Geology of a part of the south flank of the Seminoe Mountains, Carbon County, Wyoming. Unpublished M.S. thesis, University of Wyoming.

Bergh, S. G. & Snoke, A. W. 1992. Polyphase Laramide deformation in the Shirley Mountains, south-central Wyoming foreland. *Mountain Geol.* **29**, 85–100.

Blackstone, D. L. 1983. Laramide compressional tectonics, southeastern Wyoming. *Contr. Geol., Univ. Wyoming* **22**, 1–38.

Boyer, S. E. 1986. Styles of folding within thrust sheets: examples from the Appalachian and Rocky Mountains of the U.S.A. and Canada. *J. Struct. Geol.* **8**, 325–339.

Brown, W. G. 1988. Deformational style of Laramide uplifts in the Wyoming foreland. In: *Interaction of the Rocky Mountain Foreland and the Cordilleran Thrust Belt* (edited by Schmidt, C. J. & Perry, W. J., Jr). *Mem. geol. Soc. Am.* **171**, 53–64.

Chapman, T. J. & Williams, G. D. 1984. Displacement-distance methods in the analysis of fold–thrust structures and linked fault systems. *J. geol. Soc. Lond.* **141**, 121–128.

Charlesworth, H. A. K. & Gagnon, L. G. 1985. Intercutaneous wedges, the triangle zone and structural thickening of the Mynheer coal seam at Coal Valley in the Rocky Mountain foothills of central Alberta. *Bull. Can. Petrol. Geol.* **33**, 22–30.

Chester, J. & Chester, F. 1990. Fault propagation folds above thrusts with constant dip. *J. Struct. Geol.* **12**, 903–910.

Cooper, H. T. 1951. Geology of the western Seminoe Mountains. Unpublished M.S. thesis, University of Wyoming.

Cowie, P. A. & Scholz, C. H. 1992. Physical explanation for displacement-length relationship of faults using a post-yield fracture mechanics model. *J. Struct. Geol.* **14**, 1133–1148.

Currie, J. B., Patnode, H. W. & Trump, R. P. 1962. Development of folds in sedimentary strata. *Bull. geol. Soc. Am.* **73**, 655–674.

Eisenstadt, G. & De Paor, D. G. 1987. Alternative model of thrust-fault propagation. *Geology* **15**, 630–633.

Ellis, M. A. & Dunlap, W. J. 1988. Displacement variation along thrust faults: implications for the development of large faults. *J. Struct. Geol.* **10**, 183–192.

Erslev, E. A. 1986. Basement balancing of Rocky Mountain foreland uplifts. *Geology*, **14**, 249–262.

Erslev, E. A. 1991. Trishear fault propagation folding. *Geology* **19**, 617–620.

Hausel, W. D. & Jones, R. W. 1984. Self-guided tour of the geology of a portion of southeastern Wyoming. *Geol. Surv. Wyoming Pub. Info. Circ.* **21**.

Hennings, P. H. & Spang, J. H. 1987. Sequential development of Dry Fork Ridge anticline, northeastern Bighorn Mountains, Wyoming and Montana. *Contr. Geol., Univ. Wyoming* **25**, 73–93.

Jamison, W. R. 1987. Geometric analysis of fold development in overthrust terranes. *J. Struct. Geol.* **9**, 207–219.

Kraig, D. H., Wiltschko, D. V. & Spang, J. H. 1988. The interaction of the Moxa arch (La Barge platform) with the Cordilleran thrust belt, south of Snider basin, southwestern Wyoming. In: *Interaction of the Rocky Mountain Foreland and the Cordilleran Thrust Belt* (edited by Schmidt, C. J. & Perry, W. J., Jr). *Mem. geol. Soc. Am.* **171**, 395–410.

McConnell, D. A. & Wilson, T. G. 1993. Linkage between deformation of basement rocks and sedimentary rocks in basement-involved foreland folds. In: *Basement Behavior in Rocky Mountain Structures* (edited by Schmidt, C. J., Chase, R. B. & Erslev, E. A.). *Spec. Pap. geol. Soc, Am.* **280**, 319–333.

Miller, E. W. & Lageson, D. R. 1993. Influence of basement foliation attitude on geometry of Laramide basement deformation, southern Bridger Range and northern Gallatin Range, Montana. In: *Basement Behavior in Rocky Mountain Structures* (edited by Schmidt, C. J., Chase, R. B. & Erslev, E. A.). *Spec. Pap. geol. Soc. Am.* **280**, 73–88.

Mitra, S. 1990. Fault-propagation folds: Geometry, kinematic evolution, and hydrocarbon traps. *Bull. Am. Ass. Petrol. Geol.* **74**, 921–945.

Muraoka, H. & Kamata, H. 1983. Displacement distribution along minor fault traces. *J. Struct. Geol.* **5**, 483–495.

Narr, W. & Suppe, J. 1989. Kinematics of low-temperature, basement-involved compressive structures. *Geol. Soc. Am. Abs. w. Prog.* **21**, 137.

Schmidt, C. J., Genovese, P. W. & Chase, R. B. In press. Role of basement and cover rock behavior in kinematics of the Rocky Mountain foreland folds. In: *Basement Behavior in the Rocky Mountain Foreland Structures* (edited by Schmidt, C. J., Chase, R. B. & Erslev, E. A.). *Spec. Pap. geol. Soc. Am.* **280**, 1–44.

Shoemaker, R. W. 1936. The geology of the Shirley and Seminoe Mountains area, Carbon county, Wyoming. Unpublished M.S. thesis, University of Wyoming.

Spang, J. H., Evans, J. P. & Berg, R. R. 1985. Balanced cross sections of small fold-thrust structures. *Mountain Geol.* **22**, 41–46.

Stearns, D. W. 1971. Mechanisms of drape folding in the Wyoming province. *Wyoming Geol. Ass. Guide, 23rd Ann. Field Conf.*, 125–143.

Suppe, J. & Medwedeff, D. A. 1984. Fault-propagation folding. *Geol. Soc. Am. Abs. w. Prog.* **16**, 670.

Suppe, J. & Medwedeff, D. A. 1990. Geometry and kinematics of fault-propagation folding. *Eclog. geol. Helv.* **83**, 409–454.

Williams, G. D. & Chapman, T. J. 1983. Strains developed in the hanging walls of thrusts due to their slip/propagation rate: a dislocation model. *J. Struct. Geol.* **6**, 563–571.